

Invited talk at IAGUSP Workshop on Young Galaxies and QSO Absorbers

Cosmic Minivoids in the Intergalactic Medium

Avery Meiksin

*Department of Astronomy and Astrophysics, University of Chicago,
5640 S. Ellis Ave., Chicago, IL 60637; meiksin@oddjob.uchicago.edu*

Abstract. The Gunn-Peterson effect, absorption of Ly α photons by a homogeneous component of the intergalactic medium (IGM), potentially provides a test of Big Bang Nucleosynthesis (BBN). With a lower limit on the UV radiation field estimated from the contribution due to QSOs, a measurement of the Ly α opacity of the intergalactic medium would permit the derivation of a lower bound to the baryonic density of the universe. The effect, however, has continually eluded a convincing detection, both in H I and He II, despite extensive searches. Recent cosmological hydrodynamical simulations of structure formation in the intergalactic medium suggest an explanation for its absence. In a Cold Dark Matter dominated cosmology, the fragmentation of the baryons is nearly complete, leaving a negligible remnant to comprise a smoothly distributed component. The fragmentation extends even into regions that are underdense, where it gives rise to most of the optically thin H I systems and nearly all of the He II systems, both thin and saturated. The result is a Ly α opacity from a smooth IGM that is suppressed by over two orders of magnitude from the BBN value.

1. Introduction

Soon after the identification of the first QSO, Gunn & Peterson (1965) recognized that its spectrum could be used to place a stringent limit on the density of neutral hydrogen in the intergalactic medium (IGM). Photons blueward of the frequency of Ly α will be absorbed by neutral hydrogen en route to the observer in an expanding homogeneous IGM while photons redward will be transmitted (Field 1959). Hence, a step in the spectrum of a QSO is expected shortward of its Ly α emission line. Gunn and Peterson found a step corresponding to an opacity of $\sim 1/2$, and a neutral comoving H I density of $n_{\text{HI}} \approx 2 \times 10^{-12} \text{ cm}^{-3}$. This is only a tiny fraction of the density of hydrogen in galaxies today. Their inference was that the IGM must be highly ionized. The detection of absorption by a homogeneous ionized component, the ‘‘Gunn-Peterson effect’’, would have important implications for cosmology. If the gas is photoionized, then the equation of photoionization equilibrium may be solved for the baryon density of the IGM, given an estimate of the ionizing radiation field. A lower bound on the radiation field may be placed by summing the contribution due to QSOs, which would then permit a lower bound to be set on the density of the IGM. This would be a direct test of Big Bang Nucleosynthesis (BBN).

Subsequently, however, more detailed spectra revealed a host of absorption lines shortward of Ly α . These were identified by Lynds (1971) as Ly α absorption by intervening discrete absorbers, the Ly α forest. The original opacity measured by Gunn and Peterson could be accounted for by the forest. Because the forest is clumped, it is not possible to solve for the baryon density of the IGM independently of a cloud model. Searches since then for absorption by a homogeneous component of the IGM (e.g., Steidel & Sargent 1987), led to similar results: all the absorption could be accounted for by the Ly α forest. The homogeneous unclustered intergalactic medium expected from Big Bang nucleosynthesis has continued to evade detection. Recent numerical hydrodynamical computations of structure formation in Cold Dark Matter (CDM) dominated cosmologies suggest an explanation. These simulations show that all the baryons undergo condensation into discrete systems, even when the density of the system is less than the cosmic mean. These systems give rise to absorption lines that are optically thin at line center, and form in regions a few megaparsecs across that are themselves underdense, “cosmic minivoids.”

2. Baryons Lost

The Ly α opacity of homogeneously distributed intergalactic hydrogen photoionized by an ambient metagalactic radiation field is

$$\tau_\alpha \simeq 0.18 h_{50}^{-1} T_4^{-0.75} (\Omega_D h_{50}^2)^2 (1+z)^5 (1+2q_0z)^{-1/2} \Gamma_{\text{HI},-12}^{-1}, \quad (1)$$

where Ω_D is the total baryonic density of the diffuse homogeneous component in terms of the closure density, T_4 is the temperature of the neutral hydrogen in units of 10^4 K, $\Gamma_{\text{HI},-12}$ is the photoionization rate of the neutral hydrogen in units of 10^{-12} s^{-1} , q_0 is the cosmological deceleration parameter, and h_{50} is the Hubble constant in units of $50 \text{ km s}^{-1} \text{ Mpc}^{-1}$. In the redshift range $2 < z < 3$, the contribution of QSOs to the photoionizing background gives $\Gamma_{\text{HI},-12} \approx 1$, with an uncertainty of perhaps a factor of 2–3 (Meiksin & Madau 1993; Haardt & Madau 1996). By $z = 4$ this value may decline by a factor of 2, and by a factor of 20 by $z = 5$, although the QSO counts become increasingly uncertain at these high redshifts. The baryon density due to BBN is estimated to lie in the range $0.04 \lesssim \Omega_b h_{50}^2 \lesssim 0.08$ (2σ , Copi et al. 1995), consistent (though just barely!) with recent D/H measurements in intergalactic gas clouds (Tytler et al. 1996; Rugers et al. 1996). The expected IGM opacity is thus $\tau_\alpha \approx 0.15$ at $z = 3$ and 0.8 at $z = 4$. These values greatly exceed current (2σ) limits. Steidel & Sargent (1987) find $\tau_\alpha < 0.08$ at $z \approx 3$, while Giallongo et al. (1994) find $\tau_\alpha < 0.08$ at $z \approx 4.3$, although perhaps a more conservative upper limit is that of Jenkins & Ostriker (1991) of $\tau_\alpha < 0.6$ at $z \approx 4$.

The conflict between the expected and measured upper limits may be alleviated by postulating radiation sources in addition to QSOs, like stars or decaying particles, or if a substantial fraction of high redshift QSOs were missed in optical surveys due to obscuration by dust in intervening absorbers (Fall & Pei 1993). An increase by a factor of up to 10 would be consistent with the proximity effect (Bajtlik et al. 1988), although smaller values derived from the proximity effect may be favored (Espey 1993). Alternatively, Meiksin & Madau (1993) suggested that the conflict may indicate a very clumpy IGM. They argued that

a large fraction of the baryons may be contained in the Ly α forest, given the observed numbers and size constraints of the absorbers. Their estimate was $0.002 < \Omega_{\text{Ly}\alpha} h_{50} < 0.05$ for the density parameter of baryons in the forest.

3. Numerical Simulations

It has recently become possible to compute the growth of structure in the IGM using combined N-body/hydrodynamics numerical simulations. Unlike galaxy formation, the evolution of the IGM is a relatively “clean” problem since metal cooling is negligible and feedback effects from star formation are arguably unimportant, or at most only affect the ionizing radiation field. Within the context of a given cosmology and primordial power spectrum, it is thus possible to treat the calculation as an initial value problem, without the need for introducing additional physical processes “by hand.”

Several groups have performed simulations of the IGM using a variety of techniques, and all have had remarkable success in reproducing the principal observed properties of the Ly α forest (Cen et al. 1994; Zhang et al. 1995; Hernquist et al. 1996; Miralda-Escudé et al. 1996). An unexpected finding of these calculations is that the absorbers arise predominantly in sheets and filaments that form coherent structures over scales of a few megaparsecs, with a typical thickness of a few hundred kiloparsecs. These calculations readily reproduce the observed near power-law column density distribution for the forest over the range $13 < \log N_{\text{HI}} < 17$.

In this talk, I present results from a simulation of the IGM in a Cold Dark Matter dominated cosmology (Zhang et al. 1996a,b). Standard CDM is able to match the clustering properties of material from galaxy cluster scales down, although some variant of the model is required to match to the fluctuations measured by *COBE* on larger scales. The simulations are performed in a flat cosmology with no cosmological constant, and $h_{50} = 1$. The normalization of the power-spectrum is given by $\sigma_8 = 0.7$. Since the neutral density of individual clouds scales like $\Omega_b h_{50}^2 / \Gamma_{\text{HI}}$, the counts of objects depend on the magnitude of the radiation field. The results presented below are for the radiation field determined by Haardt & Madau (1996). The hydrodynamics is solved on an Eulerian grid, with a comoving resolution of 75 kpc on a top grid of comoving size 9.6 Mpc. The behavior of the gas is resolved in a second subgrid, centered in the top grid and with a resolution 4 times greater. The Eulerian nature of the calculation has the important advantage over Lagrangian schemes of being able to resolve structures in underdense regions. These structures will be shown to be crucial for interpreting the amount of absorption by diffuse H I and especially He II gas in the IGM. Further details of the simulation are provided in Zhang (1996) and Zhang et al. (1996a, b).

4. Baryons Regained

Figure 1 shows the column density distribution of the clouds from the simulation. The clouds are found using a deblending algorithm for the lines, essential to avoid undercounting weak optically thin systems (Zhang et al. 1996a). The column densities are computed by fitting Voigt profiles to the lines. The agreement with

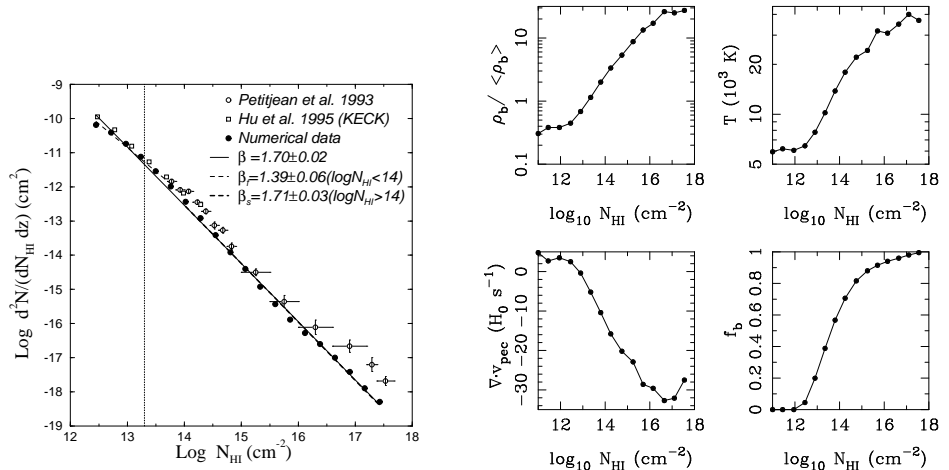


Figure 1. (*Left panel*) The distribution of HI column density at $z = 3$. The dotted line marks the division between optically thin and optically thick systems at line-center, for $b = 15 \text{ km s}^{-1}$. (*Right panel*) The mean baryon density, cloud temperature, peculiar velocity divergence, and cumulative baryon distribution as a function of HI column density.

the observed distribution is amazingly good, as was found by the other groups for the optically thick systems, having H I column densities $\log N_{\text{HI}} > 13.3$ for a Doppler parameter of 15 km s^{-1} . Here, we are able to demonstrate that the power-law behavior persists for optically thin systems as well, in agreement with Keck measurements of the forest (Hu et al. 1995).

The simulations reveal strong correlations between the cloud physical properties and column density (Zhang et al. 1996a,b). As shown in the right panels of Figure 1, the higher column density systems tend to be dense and warm, becoming more rarefied and cool toward lower values. Most of the baryons in the universe, 60%, are found to reside in the optically thick absorbers. This fact alone is able to reconcile the BBN estimate for the density of the IGM with the low Gunn-Peterson limits and a QSO-dominated ionizing UV background, since the $\text{Ly}\alpha$ opacity of a homogeneous component of the IGM would now be reduced by more than a factor of 5.

The IGM, however, is found to fragment into even lower column density systems (Hu et al. 1995). While this may not be surprising at first glance, a comparison with the minimal column density that could result from Jeans instability reveals a problem. A cloud with an internal density ρ_b that is optically thin at the Lyman edge and in ionization equilibrium with the metagalactic radiation field will have a neutral hydrogen density of $n_{\text{HI}} \simeq 5.0 \times 10^{-15} \text{ cm}^{-3} (\rho_b / \bar{\rho}_b)^2 (1+z)^6 T_4^{-0.75} \Gamma_{\text{HI},-12}^{-1}$, where $\bar{\rho}_b$ is the cosmic mean baryon density, here taken to correspond to $\Omega_b h_{50}^2 = 0.05$. The baryonic Jeans length in a medium of mixed dark matter and baryons is $\lambda_J = 2\pi(2/3)^{1/2} c_s (1+z)/H(z)$, where c_s is the sound speed of the baryons associated with a linear perturbation and $H(z)$ is the Hubble constant at redshift z (e.g., Bond & Szalay 1983). For an isothermal perturbation, $\lambda_J \simeq 1 \text{ Mpc } h_{50}^{-1} T_4^{1/2} (1+z)^{-1/2}$, or about 600 kpc at $z = 3$. This

gives a minimal column density due to Jeans instability of $\log N_{\text{HI}} \simeq 13.5$ at $z = 3$. The collapse of the system would result in an even larger neutral column density because of the increase in the recombination rate due to the increased density. Supposing that discrete features may arise only from Jeans unstable systems, one might then expect that lower column density systems cannot form. The detection of the low column density systems becomes even more perplexing on noticing the internal cloud densities required. Observations of the neighboring lines-of-sight to the images of the lensed QSO candidate HE 1104–1805 (Smette et al. 1995), place a lower limit of 100 kpc on the size of the systems with $\log N_{\text{HI}} > 13.2$. For $z > 3.5$, such systems will be underdense, $\rho_b/\bar{\rho}_b < 1$. The existence of the optically thin systems thus poses a puzzle.

Figure 1 shows that in the simulation, optically thin features do form, and they indeed originate in clouds that are underdense. The fragmentation of the IGM is complete. At most a few percent of the baryons remain outside discrete systems to comprise a homogeneous diffuse component. Insight into the origin of the optically thin systems is provided by the simulation. I first discuss, however, a simple model that offers a possible resolution to the difficulty of their occurrence.

5. Cosmic Minivoids

5.1. Spherical Model

In an open universe, the growth of linear density perturbations “freezes out” at an early stage, at an epoch given roughly by $1 + z_f \approx \Omega^{-1} - 1$ (Peebles 1980). While bound systems will continue to collapse, unbound systems will expand like the expansion of the universe. In a flat universe, similar behavior will occur in a region that is locally underdense, since any perturbation inside will find itself in a locally open universe.

Consider now a region that is slightly underdense in an Einstein-deSitter universe, a cosmic void. Because it is underdense, it will grow in size slightly faster than the surrounding cosmic expansion, increasing its underdensity. Initially ripples within the void may grow, just as those outside, but once the void becomes sufficiently underdense, their growth will slow. Those that are bound will continue to collapse as they become nonlinear. But ripples that were originally underdense, but not as strongly underdense as the background void, will freeze (relative to the cosmic background) into discrete structures within the void. These underdense systems would give rise to discrete optically thin absorption features after exposure to an ionizing radiation field, even though they are unbound.

This is illustrated in Figure 2. An initially underdense compensated spherical perturbation of comoving radius 3 Mpc is shown expanding in an Einstein-deSitter universe, with $h_{50} = 1$ and $\Omega_b = 0.08$. The evolution of the dark matter and the baryons is integrated as in Meiksin (1994). At the center of the underdense region the density is initially raised slightly above the level of the void (in a growing mode), but still below the cosmic average density. A photoionizing radiation field is turned on at $z = 6$, increasing slowly with time (model ED of Meiksin & Madau 1993). A discrete absorption feature results along a line-of-sight passing through the void center, with a column density of $\log N_{\text{HI}} = 13.1$

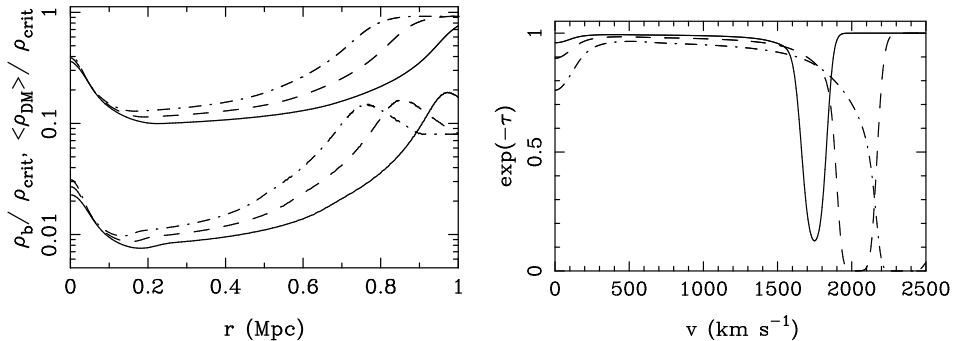


Figure 2. (*Left panel*) The evolution of density in a spherical minivoid. Upper curves show the dark matter density and the lower curves show the baryon density, both normalized by the cosmic mean density. The curves are shown at $z = 3$ (*solid*), $z = 3.5$ (*dashed*), and $z = 4$ (*dot-dashed*). (*Right panel*) The spectrum for a line-of-sight passing through the center of the minivoid. Optically thin absorption systems develop both at the minivoid center and at its boundary. The velocity is in the observer’s frame. The solutions demonstrate that discrete absorption features may arise from a region that is Jeans stable.

at $z = 4$. The perturbation is nearly frozen, with only a small decrease in the baryon overdensity due to pressure gradients, despite the fact that the system is Jeans stable. The reason is that the expansion velocity of the void from its center to the edge of the feature somewhat exceeds the isothermal sound speed of the gas. The feature is transient, but its expansion is dominated by the flow in the void rather than by thermal pressure. A second feature appears near the void boundary. This feature results from the collisional nature of the gas, which is compressed near the wall of the void where it meets the more slowly expanding external IGM. (This results in a positive bias for the baryons just within the void boundary.) Both mechanisms give rise to optically thin absorption features.

5.2. Simulation Results

The numerical simulation displays elements similar to this simple model. The underdense gas is indeed expanding faster than the cosmic rate, as shown by its positive peculiar velocity divergence in Figure 3. The structures form in regions a few comoving megaparsecs across. These minivoids are bordered by the collapsed filaments and sheets that give rise to the optically thick systems (Figure 3). By contrast, almost all of the He II systems, even those that are saturated, form in the minivoids. Because the effective opacity due to line-blanketing is dominated by features that are just becoming saturated (Madau & Meiksin 1994), the He II Ly α opacity in a QSO spectrum serves as a probe of the structure of the minivoids. A more complete description of the He II absorption and the cloud structure is provided in Zhang et al. (1996a, b).

These results admit a nontrivial consistency check based on the total opacity of the optically thin systems. While equation (1) may not be inverted to solve for Ω_D in the presence of clumping, a lower limit to the cosmic baryon density

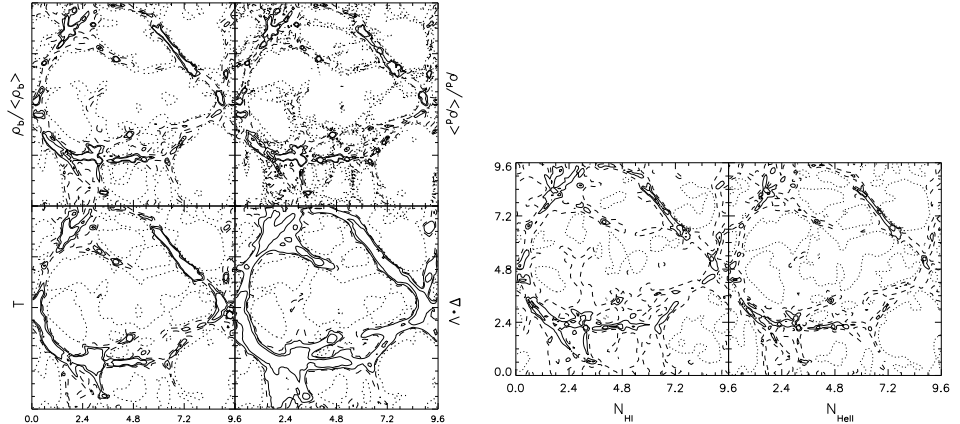


Figure 3. Contour plots of a 150 kpc thick slice of the simulation box at $z = 3$, centered on a minivoid. The box size is 9.6 comoving Mpc. (*Left panels*) The baryon (top left) and dark matter (top right) contour levels are 0.5 (*dotted*), 1 (*dashed*), 3 (*thin solid*), and 5 (*thick solid*). The temperature contours, in units of 10^3 K, are 6 (*dotted*), 10 (*dashed*), 14 (*thin solid*), and 20 (*thick solid*). The peculiar velocity divergence contours are, in units of the Hubble constant at $z = 3$, 5 (*dotted*), 0 (*dashed*), -3 (*thin solid*), and -15 (*thick solid*). The low density region bordered by the filaments exhibits density fluctuations with positive velocity divergence. These fluctuations give rise to discrete optically thin absorption features. (*Right panels*) Contour plots of the HI and HeII column densities. The contour plots are at $\log N_{\text{HI}} = 12$ (*dotted*), 13 (*dashed*), 14 (*thin solid*), and 15 (*thick solid*), and at $\log N_{\text{HeII}} = 14$ (*dotted*), 15 (*dashed*), 16 (*thin solid*), and 17 (*thick solid*) (although radiative transfer has been ignored for HeII). The minivoid is populated by optically thin HI systems, and saturated HeII systems.

may be obtained when the absorbers are optically thin and underdense. Taking τ_α to refer to the net stochastic absorption of the optically thin systems, Ω_D may be interpreted as the spatially averaged *rms* baryon density of the optically thin systems. (This is true only for optically thin clouds. See Jenkins & Ostriker 1991 for the case including optically thick absorbers.) If the internal density of the clouds is less than the cosmic mean, Ω_D provides a lower bound to the average cosmic baryon density. Counting the lines in Hu et al. (1995) for which the line-center Ly α opacity is less than 0.5, and doubling to account for incompleteness (as discussed in Hu et al.), gives $\tau_\alpha \approx 0.08$ for the optically thin systems. This yields a lower limit for the cosmic baryon density of $\Omega_b > 0.02h_{50}^{-3/2}$, consistent with the value $\Omega_b = 0.06$ adopted in the simulation.

The trends in Figure 1 permit a determination of the mass distribution of the clouds. Over the column density range $12.5 < \log N_{\text{HI}} < 14.5$, the internal baryon density of the clouds scales according to $\rho_b / \bar{\rho}_b \simeq N_{\text{HI},13}^{1/2}$, where $N_{\text{HI},13}$ is the column density in units of 10^{13} cm^{-2} . The neutral fraction scales like $f_{\text{HI}} \equiv n_{\text{HI}}/n_{\text{H}} \simeq 3.8 \times 10^{-6} [(1+z)/4]^3 T_4^{-0.75} \Gamma_{\text{HI},-12}^{-1} N_{\text{HI},13}^{1/2}$. (Note that these

relations imply a roughly constant size for the absorbers of ~ 100 kpc over this column density range.) The observed number of absorption systems is $\partial^2 N / \partial N_{\text{HI}} \partial z \approx 6 \times 10^{-13} N_{\text{HI},13}^{-1.5} (1+z)^{2.5}$ (Hu et al. 1995). These results may be combined to derive the contribution of the Ly α forest to the closure density,

$$\Omega_{\text{Ly}\alpha} = \frac{1.4 m_{\text{H}} H_0}{\rho_{\text{crit}} c} \int dN_{\text{HI}} \frac{N_{\text{HI}}}{f_{\text{HI}}} \frac{\partial^2 N}{\partial N_{\text{HI}} \partial z} (1+z)^{5/2} \propto \log \left(\frac{N_{\text{HI,max}}}{N_{\text{HI,min}}} \right). \quad (2)$$

Most of the baryons lie in the column density range $12.5 < \log N_{\text{HI}} < 14.5$, distributed equally per decade in column density, in accordance with Figure 1. Only a small fraction, less than 5%, is found to reside in systems with column densities smaller than $10^{12.5} \text{ cm}^{-2}$. Since the density of neutral hydrogen scales like the square of the baryon density, according to this model *the reason it has been so difficult to detect the Gunn-Peterson effect is that the Ly α opacity associated with a homogeneous component of the IGM has been suppressed by at least two orders of magnitude compared with the BBN value due to fragmentation.*

6. Observational Verification

To date, most of the evidence supporting the results of the simulations is circumstantial. The strongest evidence is provided by the large cloud sizes inferred from neighboring lines-of-sight to QSOs (Smette et al. 1995; Fang et al. 1996), however the filamentary nature of the absorbers found in the simulations has yet to be demonstrated. The possibility that the clouds are giant spheres (though perhaps unlikely), cannot yet be excluded. Indeed, the higher column density systems ($\gtrsim 10^{16} \text{ cm}^{-2}$) may still well arise from moderate sized spheroidal minihalos (Rees 1986; Ikeuchi 1986). (See Charlton et al. 1996 for a discussion of the observational implications of the simulations for neighboring line-of-sight statistics.) A strategy for demonstrating a flattened or filamentary geometry for the absorbers is to map their distribution on the sky using multiple lines-of-sight with transverse separations up to a few megaparsecs. Similarly, while the sizes and abundances of the absorbers are consistent with their being the dominant reservoir of the baryons at high redshift ($z > 2$), the uncertainties in the cloud sizes and geometry, BBN baryon density, and magnitude of the ionizing UV background preclude a definite statement.

Evidence in support of the findings of the simulations may come from an entirely different direction. Tytler et al. (1995) and Songaila & Cowie (1996) report the detection of C IV in the Ly α forest. Songaila and Cowie find a median ratio of $N_{\text{CIV}}/N_{\text{HI}} \sim 3 \times 10^{-3}$ for $15 < \log N_{\text{HI}} < 17$. The detection of C II would permit a direct estimate of the ionization parameter $U = n_{\gamma}/n_{\text{H}}$, where n_{γ} is the number density of ionizing photons and n_{H} the total internal hydrogen density of a cloud. The Haardt & Madau (1996) spectrum has a large break at the He II Lyman edge, and a spectral index of ≈ 0.5 between the hydrogen and helium Lyman edges. Thus $n_{\gamma} \simeq 1.8 \times 10^{-5} \Gamma_{\text{HI},-12}$. Using the relation above found between cloud internal density and column density, the ionization parameter for the clouds is $U \simeq 2.3 N_{\text{HI},13}^{-1/2}$ at $z = 3$. There is some question as to how close the absorbers are to photoionization thermal

equilibrium. Low column density clouds will have too low a density ($n_{\text{H}} < 10^{-4} \text{ cm}^{-3}$), to maintain photoionization thermal equilibrium, and so will be too cool (due to the adiabatic expansion of the IGM from which they arose), while infalling material in higher column density systems may be shock-heated to too high a temperature (Meiksin 1994). The temperatures are available from the simulation, and so may be used directly (Zhang et al. 1996b). Here we give indicative values for the metal ionization using CLOUDY (Ferland 1993), for which photoionization thermal equilibrium is assumed. Consider a typical cloud with a column density of $\log N_{\text{HI}} = 15.5$. Its internal hydrogen density will be $n_{\text{H}} \approx 1 \times 10^{-4} \text{ cm}^{-3}$ and its ionization parameter will be $U = 0.13$. The neutral hydrogen fraction in the cloud is $f_{\text{HI}} \approx 10^{-4.8}$, and the fractions of C IV, C II, and Si IV are $f_{\text{CIV}} \approx 10^{-1.4}$, $f_{\text{CII}} \approx 10^{-3.9}$, and $f_{\text{SiIV}} \approx 10^{-5.2}$. If the slabs are uniform, so that the metal column densities may be added for comparing with the H I, then matching to $N_{\text{CIV}}/N_{\text{HI}} \approx 0.003$ requires a carbon abundance of about 0.4% solar. Both C II and Si IV will be undetectable, with $N_{\text{CII}}/N_{\text{CIV}} \approx 3 \times 10^{-3}$ and $N_{\text{SiIV}}/N_{\text{CIV}} \approx 2 \times 10^{-5}$ (for a solar abundance ratio of Si to C). A detection of C II matching the predicted value, however, may be made possible by stacking spectra showing C IV absorption. For a system with $\log N_{\text{HI}} = 16.5$, the situation improves. The simulations predict $U \simeq 0.04$, which gives $f_{\text{HI}} \approx 10^{-4.3}$, $f_{\text{CIV}} \approx 10^{-0.7}$, $f_{\text{CII}} \approx 10^{-2.1}$, and $f_{\text{SiIV}} \approx 10^{-2.9}$. The required carbon abundance is 0.2% solar. In this case, $N_{\text{CII}}/N_{\text{CIV}} \approx 0.04$, so that C II should be detectable, while $N_{\text{SiIV}}/N_{\text{CIV}} \approx 7 \times 10^{-4}$. It is critical that measurements be performed at high resolution to ensure that the same subcomponents of an individual Ly α cloud are compared. Songaila & Cowie (1996) report values for $N_{\text{CII}}/N_{\text{CIV}}$ in good agreement with the $\log N_{\text{HI}} = 16.5$ prediction. Their values for $N_{\text{SiIV}}/N_{\text{CIV}}$, however, are substantially higher than the estimates provided here. This suggests that there may be a second population of absorption systems not accounted for by the simulations (e.g., York et al. 1986), or that the assumption of photoionization thermal equilibrium is violated. A more careful calculation of the expected column density ratios using the simulation results must be performed to address this issue.

While much remains to demonstrate the correctness of the structure of the IGM found in the numerical simulations, the ease with which the principal observed properties of the Ly α forest are reproduced in a CDM-dominated cosmology is a compelling argument in its favor. An additional prediction of the model emphasized here is that the Gunn-Peterson effect should be absent as a consequence of the fragmentation of the baryons and dark matter in cosmic minivoids. In the future, it may be possible to test rival cosmological theories based on the properties of the IGM.

Acknowledgments. The author thanks his collaborators Peter Anninos, Mike Norman, and especially Yu Zhang, whose numerical simulation results provided the material for much of this talk, and to the conference organizers for their generous hospitality.

References

- Bajtlik, S., Duncan, R. C., & Ostriker, J. P. 1988, ApJ, 327, 570
 Bond, J. R., & Szalay, A. S. 1983, ApJ, 274, 443

- Cen, R., Miralda-Escudé, J., Ostriker, J. P., & Rauch, M. 1994, *ApJ*, 437, L9
- Charlton, J., Anninos, P., Zhang, Y., & Norman, M. 1996, *ApJ* (submitted)
- Copi, C. J., Schramm, D. N., & Turner, M. S. 1995, *ApJ*, 455, L95
- Espey, B. R. 1993, *ApJ*, 411, L59
- Fall, S. M., Pei, Y. C. 1993, *ApJ*, 402, 479
- Fang, Y., Duncan, R. C., Crofts, A. P. S., & Bechtold, J. 1996, *ApJ*, 462, 77
- Ferland, G. J. 1993, University of Kentucky Department of Physics and Astronomy Internal Report
- Field, G. B. 1959, *ApJ*, 129, 536
- Giallongo, E., et al. 1994, *ApJ*, 425, L1
- Gunn, J. E., & Peterson, B. A. 1965, *ApJ*, 142, 1633
- Haardt, F., & Madau, P. 1996, *ApJ*, 461, 20
- Hernquist, L., Katz, N., Weinberg, D. H., & Miralda-Escudé, J. 1995, *ApJ*, 457, L51
- Hu, E. M., Kim, T.-S., Cowie, L. L., Songaila, A., & Rauch, M. 1995, *AJ*, 110, 1526
- Ikeuchi, S. 1986, *Ap&SS*, 118, 509
- Jenkins, E. B., & Ostriker, J. P. 1991, *ApJ*, 376, 33
- Lynds, C. R. 1971, *ApJ*, 164, L73
- Madau, P., & Meiksin, A. 1994, *ApJ*, 433, L53
- Meiksin, A. 1994, *ApJ*, 431, 109
- Meiksin, A., & Madau, P. 1993, *ApJ*, 412, 34
- Miralda-Escudé, J., Cen, R., Ostriker, J. P., & Rauch, M. 1996, *ApJ* (submitted)
- Peebles, P. J. E. 1980, *The Large-Scale Structure of the Universe*, Princeton: Princeton University Press, § 11
- Petitjean, P., et al. 1993, *MNRAS*, 262, 499
- Rees, M. J. 1986, *MNRAS*, 218, 25P
- Rugers, M., & Hogan, C. J. 1996, *ApJ*, 459, L1
- Smette, A., Robertson, J. G., Shaver, P. A., Reimers, D., Wisotzki, L., & Koehler, T. 1995, *A&AS*, 113, 199
- Songaila, A., & Cowie, L. L. 1996, *AJ*, 112, 335
- Steidel, C. C., & Sargent, W. L. W. 1987, *ApJ*, 318, L11
- Tytler, D., et al. 1995, in *QSO Absorption Lines*, ESO Astrophysics Symposia, G. Meylan, Heidelberg: Springer, 289
- Tytler, D., Fan, X.-M., & Burles, S. 1996, *Nature*, 381, 207
- York, D. G., Dopita, M., Green, R., & Bechtold, J. 1986, *ApJ*, 311, 610
- Zhang, Y. 1996, Ph.D. thesis, University of Illinois at Urbana-Champaign
- Zhang, Y., Anninos, P., & Norman, M. L. 1995, *ApJ*, 453, L57
- Zhang, Y., Anninos, P., Norman, M. L., & Meiksin, A. 1996a, *ApJ* (in preparation)
- Zhang, Y., Meiksin, A., Anninos, P., & Norman, M. L. 1996b, *ApJ* (in preparation)